Enhanced CAR-T cell activity against solid tumors by vaccine boosting through the chimeric receptor

Leyuan Ma[1,6], **Tanmay Dichwalkar**[1], **Jason Y.H. Chang**[1], **Benjamin Cossette**[1], **Daniel Garafola**[1], **Angela Q. Zhang**[1], **Michael Fichter**[1], **Chensu Wang**[1], **Simon Liang**[1], **Murillo Silva**[1], **Sudha Kumari**[1], **Naveen K. Mehta**[1,3], **Wuhbet Abraham**[1], **Nikki Thai**[1], **Na Li**[1], **K. Dane Wittrup**[1,3,4], **Darrell J. Irvine**[1,2,3,5,6]

[1]David H. Koch Institute for Integrative Cancer Research, Massachusetts Institute of Technology, Cambridge, Massachusetts, 02139, United States.

[2]Department of Materials Science and Engineering, Massachusetts Institute of Technology, Cambridge, Massachusetts, 02139, United States.

[3]Department of Biological Engineering, Massachusetts Institute of Technology, Cambridge, Massachusetts, 02139, United States.

[4]Department of Chemical Engineering, Massachusetts Institute of Technology, Cambridge, Massachusetts, 02139, United States.

[5]Ragon Institute of Massachusetts General Hospital, Massachusetts Institute of Technology, Cambridge, Massachusetts, 02139, United States.

[6]Howard Hughes Medical Institute, Chevy Chase, Maryland, 20815, United States.

Abstract

Chimeric Antigen Receptor T cells (CAR-T) have been effective in the treatment of hematologic malignancies, but have shown limited efficacy against solid tumors. Here we demonstrate an approach to enhance CAR-T function in solid cancers by vaccine-boosting donor cells through their chimeric receptor directly *in vivo*. We designed amphiphile CAR-T ligands (amph-ligands), which upon injection trafficked to lymph nodes and decorated the surfaces of antigen presenting cells, thereby priming CAR-T in the native lymph node microenvironment. Amph-ligand boosting triggered massive CAR-T expansion, increased donor cell polyfunctionality, and enhanced anti-tumor efficacy in multiple immunocompetent mouse tumor models. We demonstrate two approaches to generalize this strategy to any chimeric antigen receptor, enabling this simple non-

HLA-restricted approach to enhanced CAR-T functionality to be applied to existing CAR-T designs.

One Sentence Summary:

Vaccine boosting enhances CAR-T cell therapy.

Main Text:

CAR-T immunotherapy targeting the CD19 antigen has produced some dramatic clinical responses in patients with leukemia and lymphoma, and includes a high proportion of durable complete remissions (1, 2). However, poor functional persistence of CAR-T cells in some patients results in disease progression (3). Despite the success of CAR-T therapy in hematological cancers, it has to date been much less effective for solid tumors, and strategies to enhance efficacy in this setting remain an important goal (4, 5). Therapeutic vaccination is one well established approach to enhance endogenous T cell responses against cancer (6). Several groups have demonstrated the concept of preparing CAR-T cells from virus-specific endogenous lymphocytes or introducing a CAR together with a second antigen receptor specific for a target peptide, and vaccinating recipients against the viral/secondary antigen to boost CAR-T therapy (7–9). However, these approaches suffer from being HLA-restricted, and the use of endogenous TCRs may be superseded by recent advances where CARs genetically targeted to the native TCR locus (thereby deleting the native TCR) have significantly enhanced activity (10).

We recently developed a strategy to target vaccines to lymph nodes by linking peptide antigens to albumin-binding phospholipid-polymers (11). Small peptides are normally rapidly dispersed into the blood following parenteral injection, but binding of amphiphile-peptides to endogenous albumin - which constitutively traffics from blood to lymph - retargets these molecules to lymph nodes. In addition to exhibiting efficient lymph trafficking, these lipid-tailed molecules can also insert into cell membranes (12). We therefore hypothesized that by attaching a small molecule, peptide, or protein ligand for a CAR to the same polymer-lipid tail, CAR ligands could be delivered by albumin to lymph nodes and subsequently partition into membranes of resident antigen presenting cells (APCs), thereby co-displaying the amphiphile-ligand (amph-ligand) from the APC surface together with native cytokine/receptor costimulation (Fig. 1A). Here we show how the dual properties of amph-ligands – lymph node targeting and membrane insertion – combine to create a booster vaccine for CAR-T cells. This amph-ligand strategy safely expands CAR-T cells *in vivo*, whilst increasing their functionality and enhancing anti-tumor activity in multiple models of solid tumors

To test the ability of amphj-ligands to functionally decorate APCs *in vivo*, we first employed a recently described "retargetable" CAR recognizing the small molecule fluorescein (FITC), which is directed against tumors by co-administration of a FITC-conjugated anti-tumor antibody (13). The anti-FITC scFv 4m5.3 (14) was fused to the CD8α transmembrane domain followed by CD28 and CD3ζ intracellular domains; the cognate amph-ligand for this murine CAR is FITC-poly(ethylene glycol) (PEG)-DSPE (amph-FITC, Fig. 1B). When

incubated with model APCs *in vitro*, amph-FITC was absorbed into the plasma membrane in a dose-dependent manner, and despite ongoing endocytosis, many molecules remained accessible to surface staining with an anti-FITC antibody (Fig. 1C–D). Amph-FITC-coated cells stimulated FITC-CAR-T cells in a dose-dependent manner and were killed by FITC-CAR-T cells (Fig. 1E–F).

Based on these findings, we next tested whether amph-FITC molecules could decorate APCs in lymph nodes (LNs) to prime FITC-CAR-T cells *in vivo*. Subcutaneous immunization of mice with free FITC did not result in accumulation in the draining LNs, whereas 10 nmol amph-FITC was detectable for 21 days (fig. S1A). Amph-FITC primarily accumulated in draining LNs, with low to negligible levels detectable in the liver, spleen and other organs (fig. S1B). Confocal imaging of LNs showed that amph-FITC initially accumulated in interfollicular regions, but partitioned onto $CD11c^+$ dendritic cells (DCs) in T cell areas over time (Fig. 2A–B, fig. S1C). Importantly, surface-displayed FITC could be detected on sorted $FITC^+CD11c^+$ cells stained with an anti-FITC antibody (Fig. 2C, fig. S1D). In contrast to the efficient amph-FITC insertion into the membranes of many LN cell types *in vitro*, surface-accessible FITC was present primarily on macrophages and $CD11c^+CD11b^+$ DCs *in vivo* (Fig. 2D, fig. S2A–C). Dendritic cells line collagen conduits carrying lymph fluid into the lymph node, and we hypothesize that the anatomic structure of LN in part dictates preferential access of these cells to amph-vax molecules entering LNs (15). This is supported by the observation that amph-FITC co-injected with a low molecular weight dextran (which is known to be transported through the LN conduit system(16)) showed substantial colocalization in fiber-like structures extending from the sinuses (fig. S2D). Immunization using amph-FITC together with the STING agonist adjuvant cyclic-di-GMP increased the duration of amph-FITC display on multiple APCs, and as expected led to upregulation of costimulatory molecules on $amph-FITC^+$ DCs (Fig. 2E, fig. S2E). Notably however, surface-accessible FITC decayed quickly and persisted on only a small fraction of cells.

To test the ability of amph-ligand immunization to expand FITC-CAR-T *in vivo*, $CD45.1^+$ FITC-CAR-T cells were transferred into lymphodepleted congenic $CD45.2^+$ recipient mice and subsequently vaccinated twice with amph-FITC and adjuvant. The CAR-T cells expanded dramatically after amph-FITC vaccination, and expansion was increased by co-administering adjuvant (Fig. 2F). For example, transfer of 5×10^4 FITC-CAR-T followed by amph-FITC vaccination with adjuvant expanded these cells to a peak of ~70% of the total $CD8^+$ T cell compartment, yielding a CAR-T population nearly double the size achieved by administering a 200-fold greater number of CAR-T cells without vaccination (Fig. 2F). By 3 weeks post-boost, the persisting CAR-T were a mixture of effector/effector memory and central memory cells (Fig. 2G). Amph-vax boosting also expanded CAR-T in lympho-replete mice; in this setting two immunizations could expand 10^6 transferred cells from undetectable levels to ~20% of the total CD8 compartment (Fig. 2H). To determine whether professional APCs played an important role in CAR-T priming by amph-ligand immunization, we depleted different cell types in LNs. CAR-T expansion in response to amph-FITC immunization was not impaired in $Batf3^{-/-}$ mice lacking cross-presenting dendritic cells, but depletion of total DCs in CD11c-DTR mice or macrophages using chlodronate liposomes led to significant reduction in CAR-T cell numbers (fig. S3A–C). In

addition, the cytokine functionality of responding CAR-T cells was reduced in all 3 settings (fig. S3A–C). In addition, *in vivo* blockade of a collection of co-stimulatory molecules expressed by APCs markedly suppressed both FITC-CAR-T expansion and cytokine functionality in response to amph-FITC immunization (fig. S3D).

A key concern with amph-ligand delivery is the potential for toxicity from CAR-T-mediated killing of decorated cells in LNs or other tissues. Consistent with the low fraction of any cell type with detectable surface FITC ligand, no significant changes in viable LN cell populations were detectable 1 day, 3 days or 14 days following amph-FITC immunization (fig. S4A–C). No changes in systemic liver enzymes, liver histopathology or CAR-T infiltration, or serum cytokine levels were observed following amph-FITC boosting (fig. S4D–I). We further evaluated the functional integrity of vaccinated LNs by administering an amph-FITC boost in the presence or absence of transferred FITC-CAR-T cells, then immunizing animals with OVA at the same site 5, 7, or 14 days later (fig. S4J). We observed decreased expansion and functionality of endogenous SIINFEKL-specific T cells immunized 5 days - but not 7 or 14 days - following amph-FITC boost, suggesting that the combination of CAR-T transfer and amph-FITC vaccination has a short-term effect on priming of endogenous T cell responses (which recovers rapidly (fig. S4K)). Due to the lack of T cell help, repeated amph-FITC immunization with adjuvant elicited no antibody response against the amph-ligand itself (fig. S5).

We next evaluated if amph-ligands could be used to prime a *bona fide* tumor antigen-specific CAR. The EGFRvIII-specific 139scFv CAR recognizes a short linear epitope derived from EGFRvIII (17). We prepared murine T cells expressing this CAR and synthesized an amph-vax molecule comprised of PEG-DSPE linked to the peptide ligand with or without an N-terminal FITC label (amph-pepvIII, Fig. 3A). Similar to amph-FITC, amph-pepvIII inserted in cell membranes *in vitro*, and amph-pepvIII-coated cells stimulated EGFRvIII-CAR-T cells (fig. S6A–B). Immunization of mice with amph-pepVIII triggered EGFRvIII-CAR-T cell proliferation *in vivo* (Fig. 3B). To test the therapeutic impact of vaccine boosting, we transduced murine CT-2A glioma cells with EGFRvIII; these cells were efficiently killed by EGFRvIII-CAR-T cells *in vitro* (fig. S6C–D). Transfer of EGFRvIII-CAR-T into lympho-depleted CT-2A-mEGFRvIII tumor-bearing mice followed by amph-pepvIII immunization expanded the CAR-T cells substantially in the periphery (Fig. 3C), with significant increases in the proportion of cells with an effector phenotype (fig. S6E), and 5–10-fold increases in CAR-T cell polyfunctionality (Fig. 3D). Amph-vax boosting greatly increased CAR-T infiltration into tumors, and these TILs expressed higher levels of granzyme B and Ki67 than unboosted CAR-T (Fig. 3E). In therapeutic studies, animals receiving both CAR-T and repeated amph-vax boosting had significantly delayed tumor growth and prolonged survival (Fig. 3F–G). Treatment with 1×10^6 CAR-T cells alone led to no long-term survivors, while this same CAR-T dose boosted by amph-vaccination eliminated tumors in a majority of animals (Fig. 3F–G). Administration of amph-pepvIII with adjuvant in the absence of CAR-T cells had no therapeutic impact (fig. S6F). EGFRvIII-CAR-T cells from vaccinated animals persisted over time, and surviving animals rejected tumor rechallenge at day 75 (fig. S6G–H). Notably, animals that rejected primary tumors following CAR-T + amph-vax boosting therapy also rejected rechallenge with parental CT-2A tumor cells lacking the ligand for the CAR-T cells, suggesting induction of an endogenous T cell response against

other tumor antigens (fig. S6I). Motivated by this finding, we evaluated the reactivity of splenocytes from CT-2A-mEGFvIII tumor-bearing mice that received CAR-T cells with or without 2 amph-pepvIII boosts. ELISPOT analysis of IFN-γ production by splenocytes cultured with parental CT-2A cells revealed a strong endogenous T cell response against parental tumors (Fig. 3H). Similar to amph-FITC vaccinated mice, no antibody response was elicited against pepvIII after 3 rounds of weekly vaccination (fig. S6J). We also evaluated the therapeutic efficacy of CAR-T plus amph-vaccination in tumor-bearing mice without lympho-depletion preconditioning. Tumor progression in animals receiving CAR-T alone was indistinguishable from animals receiving control untransduced T cells, whereas CAR-T transfer combined with amph-pepvIII immunization delayed tumor growth and prolonged animal survival (Fig. 3I–J). In both the lympho-depleted and non lympho-depleted settings, amph-vax boosting was accompanied by small transient alterations in animal body weight and minimal alterations in serum cytokine levels (fig. S6K–L). To assess the utility of amph-vax boosting with a more potent "third generation" CAR design, we generated an EGFRvIII-targeting CAR containing both CD28 and 41BB costimulatory domains. This CAR expressed well and was functional *in vitro* (fig. S7A–C). We then treated large (~50 mm^2) established CT-2A-mEGFRvIII tumors with EGFRvIII-28BBzCAR-T cells ± amph-pepvIII boosting. In this large tumor burden setting, the CAR-T cells alone had a modest impact on tumor progression, and amph-ligand boosting greatly improved tumor control and enhanced overall survival (fig. S7D–E).

While use of a peptide ligand for CAR-T cells was effective, some CARs recognize three-dimensional structural epitopes (18). As an alternative strategy to amph-ligand boost any CAR regardless of the nature of its binding domain or specificity, we devised a tandem scFv-based bispecific CAR based on recently reported designs (19): The anti-FITC scFv was fused to the N-terminal extracellular domain of a tumor-targeting CAR (TA99) recognizing the melanoma-associated antigen TRP1 (Fig. 4A–B). FITC/TRP1-CAR-T cells were activated both by amph-FITC-coated target cells and by TRP1-expressing B16F10 cells (fig. S8A), and killed TRP1^{+} target cells equivalently to mono-specific TRP1-CAR-T cells (Fig. 4C). *In vivo*, amph-FITC vaccination stimulated FITC/TRP1 bispecific CAR-T proliferation (fig. S8B). Similar to observations in the EGFRvIII system, amph-vax boosting of FITC/TRP1-CAR-T in B16F10 tumor-bearing animals led to pronounced CAR-T expansion in the periphery and increased tumor infiltration (fig. S8C–D), with minimal serum cytokine elevation and transient fluctuations in body weight after each vaccination (fig. S8E–F). While adoptive therapy with FITC/TRP1-CAR-T alone had almost no effect on B16F10 tumor progression, repeated boosting following transfer with amph-FITC led to pronounced slowing in tumor growth and extended survival (Fig. 4D–E). One resistance mechanism to CAR-T therapy is loss of surface antigen (20), but we did not observe apparent Trp1 loss upon tumor outgrowth in this model (fig. S8G–H). To assess potential autoimmune toxicity induced by amph-vax boosting, we examined thymus and skin tissues (which naturally express Trp1) from treated animals, but found no changes in histopathology or CAR-T infiltration into the thymus with amph-vax boosting (fig. S8I–K). We also assessed whether CAR-T therapy with vaccine boosting would be more effective using mixed CD4/CD8 CAR-T cells. *In vitro*, both CD4^{+} and CD8^{+} CAR-T cells were activated by culture with amph-ligand-coated target cells (fig. S8L), and similar therapeutic efficacy was observed

when B16F10 tumors were treated with CD8 vs. mixed CD4/CD8 FITC/Trp1-CAR-T cells and boosted by amph-FITC vaccination (fig. S8M–N).

To assess the broad applicability of this bispecific CAR platform irrespective of animal strain/haplotype and to evaluate treatment of metastatic disease, we prepared 4T1 tumor cells transduced to express mEGFRvIII and luciferase, modeling EGFRvIII[+] breast cancer (21) on the BALB/c background. A cognate FITC/EGFRvIII-bispecific CAR was generated, which expressed well in BALB/c T cells and was functional *in vitro* and *in vivo* (fig. S9A–D). 4T1-mEGFRvIII tumor cells were injected intravenously (i.v) into BALB/c mice to induce lung metastases, then treated with FITC/EGFRvIII-CAR-T ± amph-FITC boosting. Tumor progression as assessed by bioluminescence imaging was significantly impacted only when CAR-T cells were supplemented with amph-ligand boosting (fig. S9E), leading to prolonged survival and clearance of tumors in 2/5 animals (fig. S9F). In the CAR-T + amph-vax-treated animals that relapsed, EGFRvIII surface levels were markedly reduced, suggesting selection of antigen low/null tumor cells during therapy (fig. S9G). Finally, to verify that this bispecific CAR approach could also be utilized to boost human CAR-T, a FITC/hCD19 bispecific human CAR was constructed using the established FMC63 anti-CD19 scFv (22) and expressed in human T cells (Fig. 4F). Human FITC/hCD19-CAR-T cells were stimulated by both CD19^{+} Raji cells as well as amph-FITC-coated target cells (Fig. 4G).

Altogether, we present here a novel vaccine approach to boost CAR-T cell numbers and functionality *in vivo* with low toxicity, enabling enhanced efficacy in syngeneic solid tumor models. Although not directly evaluated here, this approach might be further enhanced by nascent strategies to improve CAR function such as insertion of the CAR into the *TRAC* locus(10). The bispecific vaccinable CAR design and amph-FITC vaccine offers a simple and universal solution to boost CAR-T cells with any antigen specificity.

Supplementary Material

Refer to Web version on PubMed Central for supplementary material.

Acknowledgements

References and Notes

1. Fesnak AD, June CH, Levine BL, Engineered T cells: the promise and challenges of cancer immunotherapy. Nat Rev Cancer 16, 566–581 (2016). [PubMed: 27550819]

2. Khalil DN, Smith EL, Brentjens RJ, Wolchok JD, The future of cancer treatment: immunomodulation, CARs and combination immunotherapy. Nat Rev Clin Oncol 13, 394 (2016). [PubMed: 27118494]

3. Guedan S et al., Enhancing CAR T cell persistence through ICOS and 4–1BB costimulation. JCI Insight 3, (2018).

4. Newick K, O'Brien S, Moon E, Albelda SM, CAR T Cell Therapy for Solid Tumors. Annu Rev Med 68, 139–152 (2017). [PubMed: 27860544]

5. June CH, O'Connor RS, Kawalekar OU, Ghassemi S, Milone MC, CAR T cell immunotherapy for human cancer. Science 359, 1361–1365 (2018). [PubMed: 29567707]

6. van der Burg SH, Arens R, Ossendorp F, van Hall T, Melief CJ, Vaccines for established cancer: overcoming the challenges posed by immune evasion. Nat Rev Cancer 16, 219–233 (2016). [PubMed: 26965076]

7. Tanaka M et al., Vaccination Targeting Native Receptors to Enhance the Function and Proliferation of Chimeric Antigen Receptor (CAR)-Modified T Cells. Clin Cancer Res 23, 3499–3509 (2017). [PubMed: 28183713]

8. Wang X et al., CMVpp65 Vaccine Enhances the Antitumor Efficacy of Adoptively Transferred CD19-Redirected CMV-Specific T Cells. Clin Cancer Res 21, 2993–3002 (2015). [PubMed: 25838392]

9. Slaney CY et al., Dual-specific Chimeric Antigen Receptor T Cells and an Indirect Vaccine Eradicate a Variety of Large Solid Tumors in an Immunocompetent, Self-antigen Setting. Clin Cancer Res 23, 2478–2490 (2017). [PubMed: 27965307]

10. Eyquem J et al., Targeting a CAR to the TRAC locus with CRISPR/Cas9 enhances tumour rejection. Nature 543, 113–117 (2017). [PubMed: 28225754]

11. Liu H et al., Structure-based programming of lymph-node targeting in molecular vaccines. Nature 507, 519–522 (2014). [PubMed: 24531764]

12. Liu H, Kwong B, Irvine DJ, Membrane anchored immunostimulatory oligonucleotides for in vivo cell modification and localized immunotherapy. Angew Chem Int Ed Engl 50, 7052–7055 (2011). [PubMed: 21688362]

13. Ma JS et al., Versatile strategy for controlling the specificity and activity of engineered T cells. Proc Natl Acad Sci U S A 113, E450–458 (2016). [PubMed: 26759368]

14. Boder ET, Midelfort KS, Wittrup KD, Directed evolution of antibody fragments with monovalent femtomolar antigen-binding affinity. Proc Natl Acad Sci U S A 97, 10701–10705 (2000). [PubMed: 10984501]

15. Sixt M et al., The conduit system transports soluble antigens from the afferent lymph to resident dendritic cells in the T cell area of the lymph node. Immunity 22, 19–29 (2005). [PubMed: 15664156]

16. Gretz JE, Norbury CC, Anderson AO, Proudfoot AE, Shaw S, Lymph-borne chemokines and other low molecular weight molecules reach high endothelial venules via specialized conduits while a functional barrier limits access to the lymphocyte microenvironments in lymph node cortex. J Exp Med 192, 1425–1440 (2000). [PubMed: 11085745]

17. Sampson JH et al., EGFRvIII mCAR-modified T-cell therapy cures mice with established intracerebral glioma and generates host immunity against tumor-antigen loss. Clin Cancer Res 20, 972–984 (2014). [PubMed: 24352643]

18. De Oliveira SN et al., A CD19/Fc fusion protein for detection of anti-CD19 chimeric antigen receptors. J Transl Med 11, 23 (2013). [PubMed: 23360526]

19. Zah E, Lin MY, Silva-Benedict A, Jensen MC, Chen YY, T Cells Expressing CD19/CD20 Bispecific Chimeric Antigen Receptors Prevent Antigen Escape by Malignant B Cells. Cancer Immunol Res 4, 498–508 (2016). [PubMed: 27059623]

20. Sotillo E et al., Convergence of Acquired Mutations and Alternative Splicing of CD19 Enables Resistance to CART-19 Immunotherapy. Cancer Discov 5, 1282–1295 (2015). [PubMed: 26516065]

21. Del Vecchio CA et al., Epidermal growth factor receptor variant III contributes to cancer stem cell phenotypes in invasive breast carcinoma. Cancer Res 72, 2657–2671 (2012). [PubMed: 22419663]

22. Kochenderfer JN et al., Eradication of B-lineage cells and regression of lymphoma in a patient treated with autologous T cells genetically engineered to recognize CD19. Blood 116, 4099–4102 (2010). [PubMed: 20668228]

23. Davila ML, Kloss CC, Gunset G, Sadelain M, CD19 CAR-targeted T cells induce long-term remission and B Cell Aplasia in an immunocompetent mouse model of B cell acute lymphoblastic leukemia. PLoS One 8, e61338 (2013). [PubMed: 23585892]

24. Ma L et al., A therapeutically targetable mechanism of BCR-ABL-independent imatinib resistance in chronic myeloid leukemia. Sci Transl Med 6, 252ra121 (2014).

25. Phan TG, Green JA, Gray EE, Xu Y, Cyster JG, Immune complex relay by subcapsular sinus macrophages and noncognate B cells drives antibody affinity maturation. Nat Immunol 10, 786–793 (2009). [PubMed: 19503106]

26. Charan J, Kantharia ND, How to calculate sample size in animal studies? J Pharmacol Pharmacother 4, 303–306 (2013). [PubMed: 24250214]

27. Moynihan KD et al., Eradication of large established tumors in mice by combination immunotherapy that engages innate and adaptive immune responses. Nat Med 22, 1402–1410 (2016). [PubMed: 27775706]

28. Adachi K et al., IL-7 and CCL19 expression in CAR-T cells improves immune cell infiltration and CAR-T cell survival in the tumor. Nat Biotechnol 36, 346–351 (2018). [PubMed: 29505028]

Author Manuscript

Author Manuscript

Author Manuscript

Author Manuscript
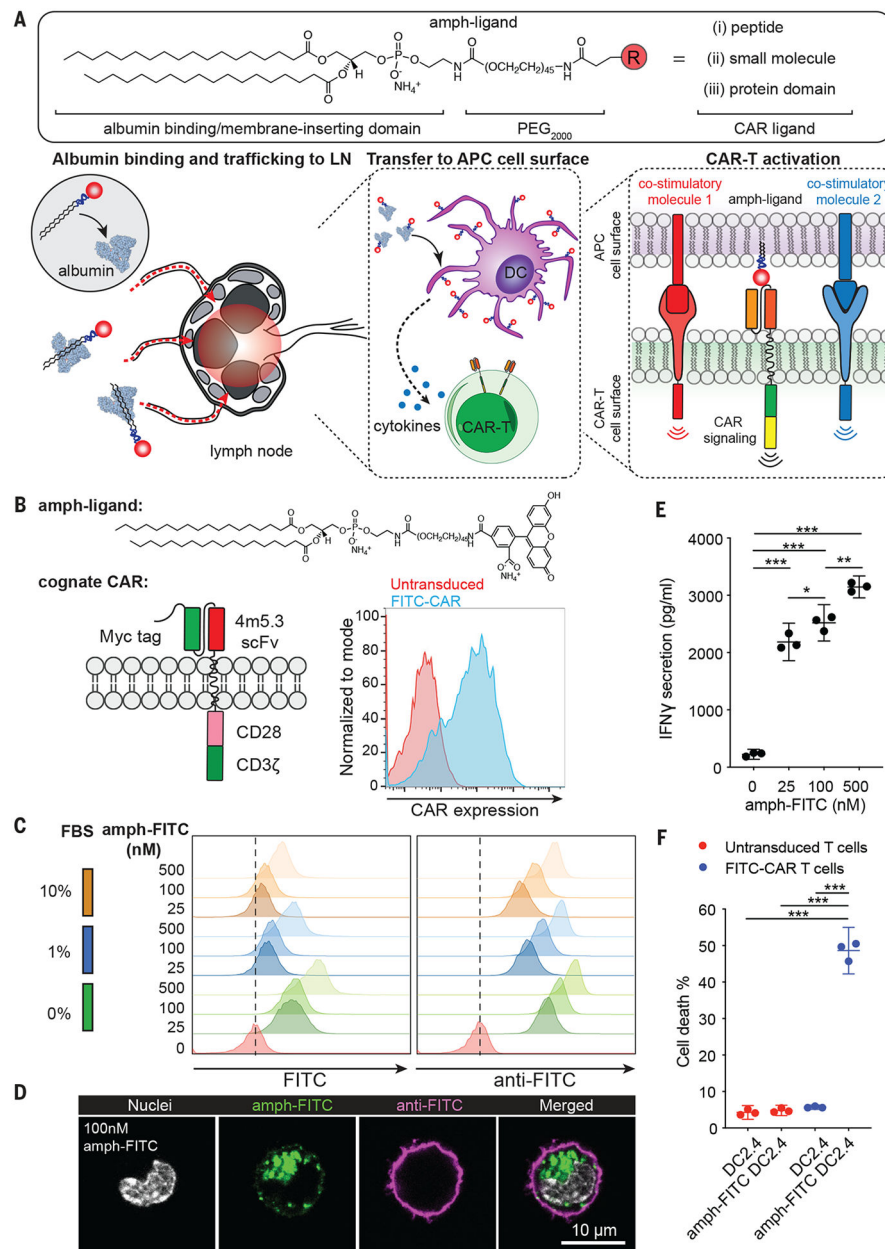
Fig. 1. Design of an amphiphile-ligand vaccine to boost CAR-T cells.
(**A**) Schematic of the general chemical structure of amph-ligands (top), and the steps in amph-ligand vaccine boosting *in vivo* (bottom): Upon injection, amph-ligands associate with albumin at the injection site and are subsequently trafficked to the draining lymph node. The amphiphiles then transfer to the membrane of lymph node-resident cells, including antigen presenting cells (APCs). CAR-T cells that encounter decorated APCs in the LN are stimulated by the surface-displayed amph-ligand as well as costimulatory receptors and cytokines produced by the APC. (**B**) Structures of amph-FITC and cognate FITC-CAR, and representative flow cytometry analysis of T cell surface expression for FITC-CAR. (**C, D**) Flow cytometry analysis at 24 hr (**C**) and confocal imaging after 30 min (**D**) of amph-FITC insertion into DC2.4 cell membranes, by direct FITC fluorescence or staining with an anti-
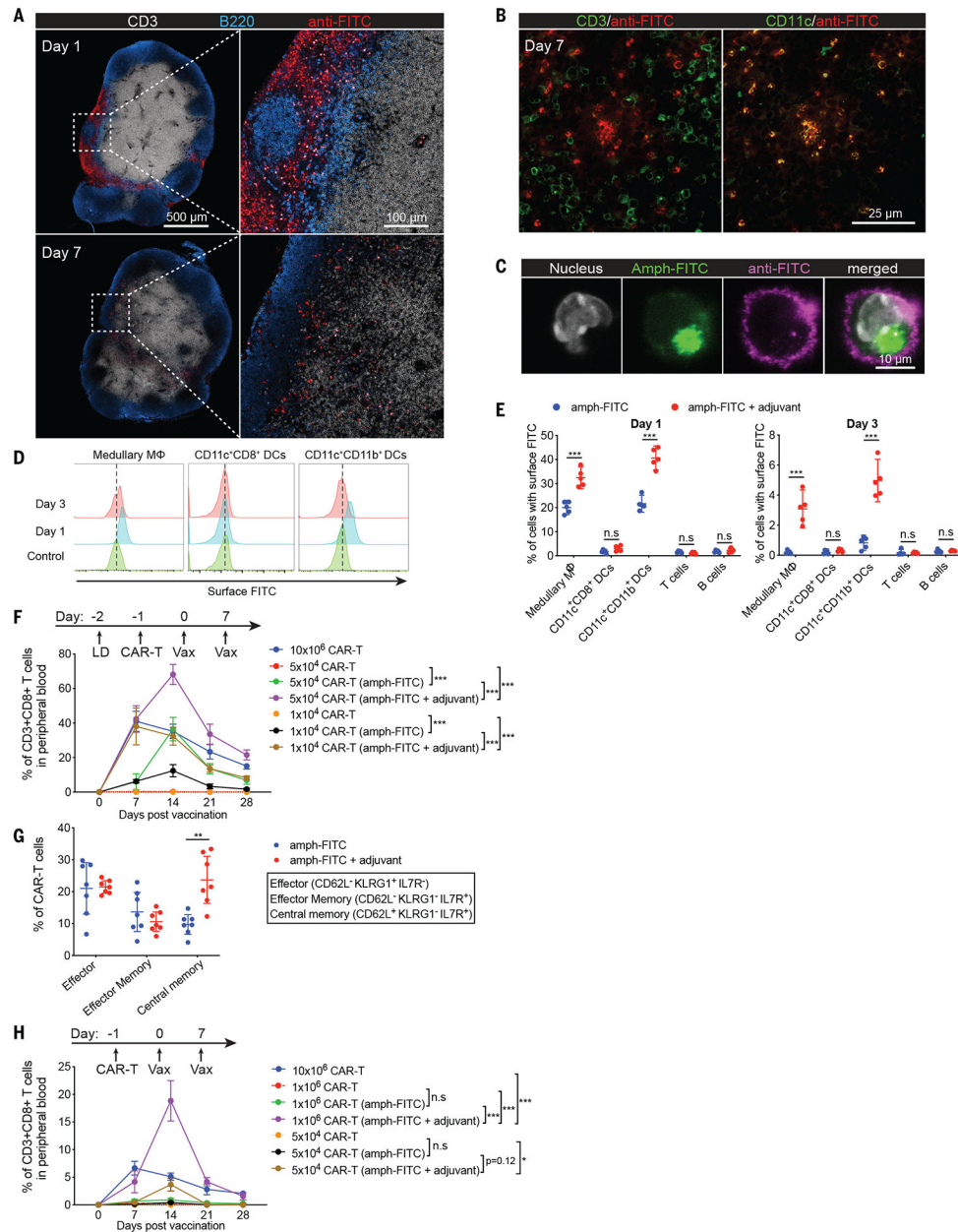
FITC antibody. (**E-F**) IFN-γ secretion (pg/ml) (**E**) and killing (% of target cell death) (**F**) of amph-FITC-coated DC2.4 cells after 6 hr co-culture with FITC-CAR-T or control untransduced T-cells at a 10:1 E:T ratio. Shown in E and F is a representative experiment with technical triplicates. P-values were determined by unpaired student's t-test. Error bars represent 95% CI; ***p<0.0001, **p<0.01, *p<0.05.

Fig. 2. Amph-ligands accumulate on lymph node APCs and prime CAR-T cells *in vivo*.
(**A-E**) C57BL/6 mice (*n*=3 animals/group for A-C, and *n*=5 animals/group for D-E) were immunized s.c. with amph-FITC and cyclic di-GMP adjuvant (**A-C, E**) or amph-FITC alone (**D, E**). Shown are histological images of LNs (**A-B**); confocal imaging of sorted amph-FITC-coated $CD11c^+$ cells isolated from LNs at 24 hours (**C**); and flow cytometry analysis of the cellular biodistribution of amph-FITC 1 or 3 days after injection (**D-E**). (**F-H**) CD45.2$^+$ C57BL/6 mice (*n*=7 animals/group) with (**F, G**) or without (**H**) prior lymphodepletion (LD) were adoptively transferred with CD45.1$^+$ FITC-CAR-T cells followed by amph-FITC vaccination. Shown are frequencies of peripheral blood CAR-T cells (**F, H**) and cellular phenotypes at day 30 (**G**). P-values were determined by unpaired student's t-test for E and G, and by RM (repeated measures) two-way ANOVA with Tukey's
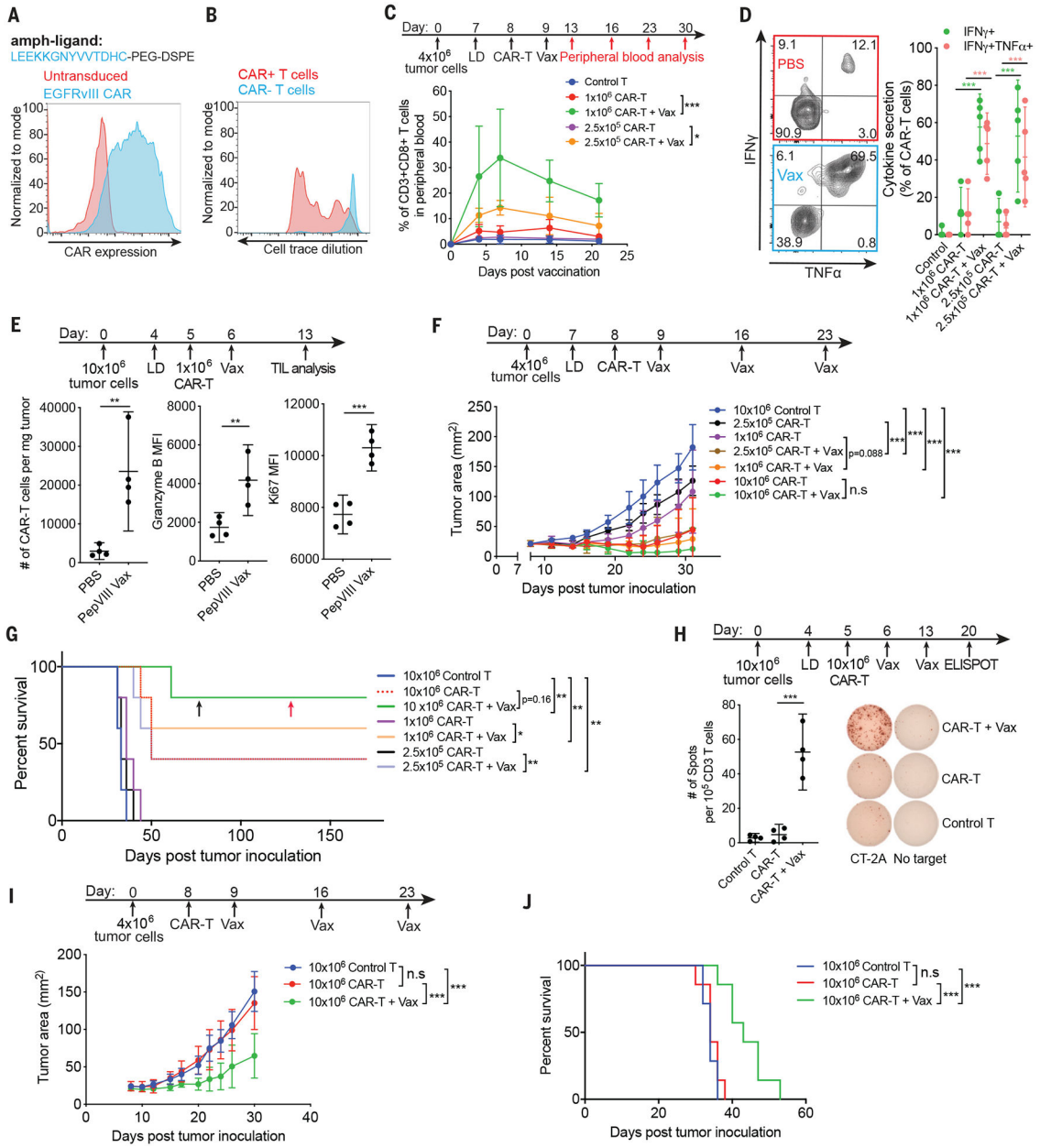
multiple comparisons test for F and H. Error bars represent 95% CI; ***p<0.001, **p<0.01, *p<0.05. n.s, not significant.

Fig. 3. Amph-peptide ligands boost CAR-T cells *in vivo* for enhanced solid tumor immunotherapy in mice.

(**A**) Structure of amph-pepVIII and surface expression of EGFRvIII CAR. (**B**) Representative histogram showing EGFRvIII-CAR-T proliferation in LNs 48 hours after amph-pepVIII vaccination (*n*=3 animals/group). (**C-D**) Expansion (**C**) and cytokine polyfunctionality at day 7 (**D**) of circulating EGFRvIII-CAR-T cells following a single amph-pepVIII immunization (*n*=5 animals/group). (**E**) Enumeration, granzyme B levels, and Ki67 levels of tumor-infiltrating EGFRvIII-CAR-T cells (*n*=4 animals/group) with or without amph-pepVIII boost. (**F-J**) Tumor growth (**F**, **I**), ELISPOT of enriched CD3+ splenocytes cultured with irradiated parental CT-2A tumor cells (**H**), and survival (**G, J**) of mEGFRvIII-CT-2A tumor-bearing mice treated with EGFRvIII-CAR-T with or without

amph-pepvIII vaccination for animals that were lympho-depleted (**F-G**, n=5 animals/group, H, n=4 animals/group) or lympho-replete (**I-J**, n=7 animals/group) prior to adoptive transfer. Black arrow indicates time of CT-2A-EGFRvIII tumor re-challenge. Red arrow indicates time of parental CT-2A tumor re-challenge. P-values were determined by unpaired student's t-test for D, E and H, by RM (repeated measures) two-way ANOVA with Tukey's multiple comparisons test for C, F and I, and by log-rank test for G and J. Error bars represent 95% CI; ***p<0.001, **p<0.01, *p<0.05. n.s, not significant.
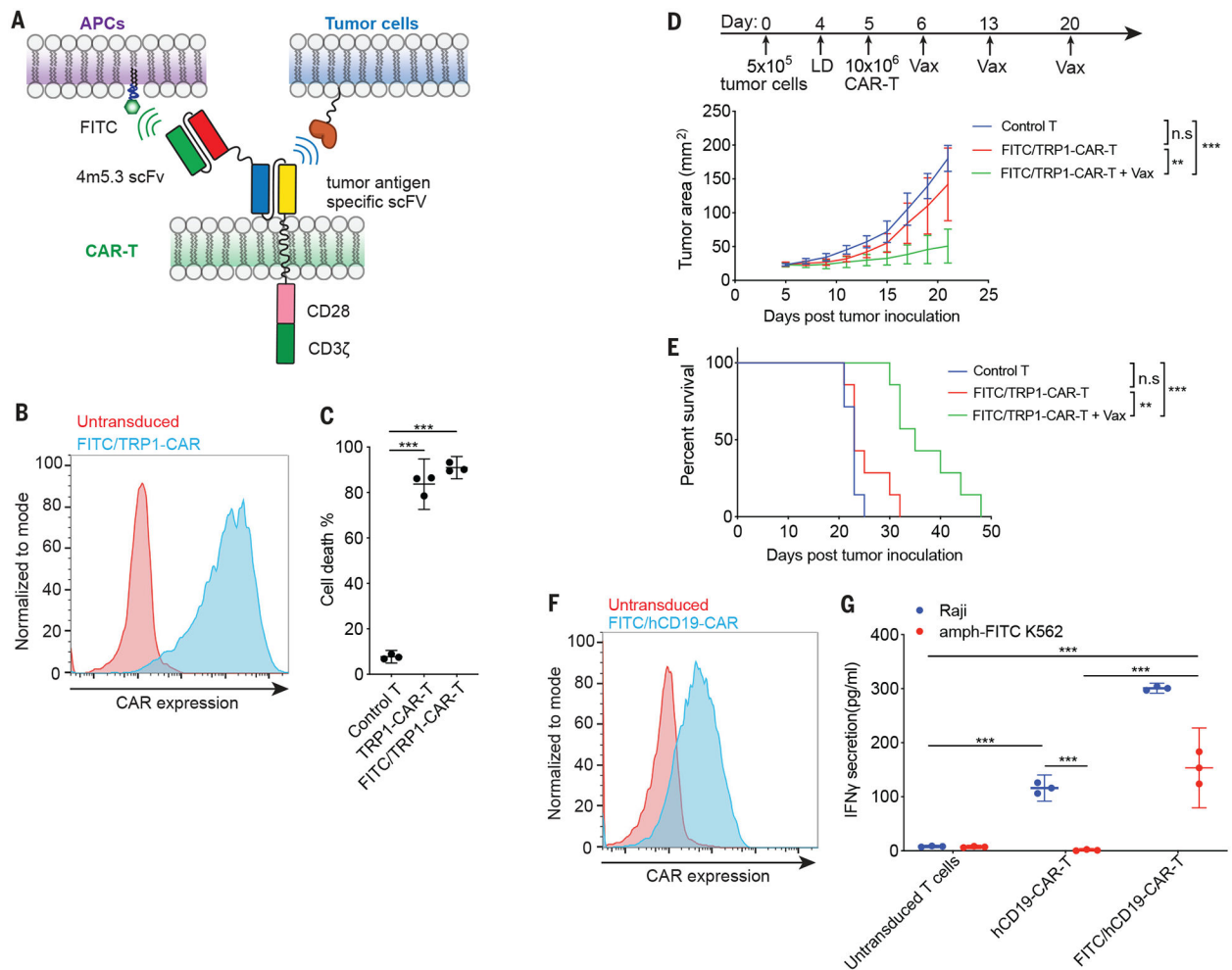
Fig. 4. Amph-FITC ligands boost the anti-tumor activity of bispecific CAR-T cells.
(**A**) Schematic of bispecific CAR design: the FITC-binding scFv 4m5.3 is fused through a short linker to a tumor antigen-specific CAR, enabling the T cell to be triggered by binding to either FITC-decorated cells or tumor cells. (**B**) Representative T cell surface expression of FITC/TRP1-CAR. (**C**) Killing of TRP1-expressing B16F10 cells *in vitro* after a 6 hr co-culture with FITC/TRP1-CAR-T, monospecific TRP1-CAR-T or control untransduced T cells at E:T of 10:1. (**D, E**) Tumor growth (**D**) and survival (**E**) of B16F10 tumor-bearing mice (*n*=7 animals/group) treated with 10×10^6 CAR-T alone or CAR-T plus amph-FITC vaccination. P-values were determined by RM (repeated measures) two-way ANOVA with Tukey's multiple comparisons test for D, and by log-rank test for E. (**F**) Surface expression of FITC/hCD19 bispecific CAR on human T cells. (**G**) FITC/TRP1 bispecific CAR-T responding to either hCD19+ Raji cells or amph-FITC-coated K562 cells as monitored by IFN-γ secretion. Shown in C and G is a representative experiment with technical triplicates. P-values were determined by unpaired student's t-test for C and G. Error bars represent 95% CI; ***p<0.0001, **p<0.01, *p<0.05. n.s, not significant.